ISSN 0023-1584, Kinetics and Catalysis, 2012, Vol. 53, No. 2, pp. 188–196. © Pleiades Publishing, Ltd., 2012.
Original Russian Text © T.P. Lyubina, E.A. Kozlova, 2012, published in Kinetika i Kataliz, 2012, Vol. 53, No. 2, pp. 197–205.

New Photocatalysts Based on Cadmium and Zinc Sulfides for Hydrogen Evolution from Aqueous Na_2S–Na_2SO_3 Solutions under Irradiation with Visible Light

T. P. Lyubina[a] and E. A. Kozlova[a, b, *]

[a] *Boreskov Institute of Catalysis, Siberian Branch, Russian Academy of Sciences, Novosibirsk, 630090 Russia*
[b] *Novosibirsk State University, Novosibirsk, 630090 Russia*
* *e-mail: kozlova@catalysis.ru*

Received August 26, 2011

Abstract—Noble metal–free, $Cd_{1-x}Zn_xS$-based photocatalysts for hydrogen evolution from aqueous solutions of sodium sulfide and sodium sulfite upon irradiation with visible light ($\lambda > 420$ nm) have been synthesized and characterized by a complex of physicochemical methods. The effects of pH and catalyst and substrate concentrations on the rate of photocatalytic hydrogen evolution have been investigated. Under the optimal conditions, the quantum efficiency of the process is up to 12.9%.

DOI: 10.1134/S0023158412020061

The rapid depletion of oil resources necessitates extensive mastering of alternative energy and raw material sources for the chemical industry. Serious attention is presently given to use of hydrogen as a fuel [1–3]. An advantage of hydrogen is its high heating value. Furthermore, the product of its combustion is water, an environmentally friendly substance. The photocatalytic decomposition of water to hydrogen and oxygen using solar energy is one of the most promising methods of hydrogen production [1–3].

The photocatalytic decomposition process can be described by Eqs. (I)–(III). Irradiation of a semiconductor photocatalyst (PC) yields charge carriers (electron e^- and hole h^+) on its surface:

$$PC + h\nu \longrightarrow PC + e^- + h^+. \quad (I)$$

In a neutral medium, an electron reduces a proton to form gaseous hydrogen:

$$2H_2O + 2e^- \longrightarrow H_2 + 2OH^-. \quad (II)$$

The photogenerated holes simultaneously oxidize water to form dioxygen:

$$2H_2O + 4h^+ \longrightarrow O_2 + 4H^+. \quad (III)$$

However, the quantum yield of this reaction is rather low because of the recombination of oxygen and hydrogen resulting from water decomposition. To enhance the efficiency of the photocatalytic hydrogen evolution, many researchers propose use of organic and inorganic donors [1–11] that can interact with the photogenerated holes, undergoing oxidation.

Cadmium sulfide was the first photocatalyst to be employed in hydrogen production by irradiation of its aqueous solutions with visible light using sulfide ions as electron donors [2–6, 8]. Cadmium sulfide is characterized by a band gap of 2.4 eV, and the positions of its valence and conduction bands are suitable for the photocatalytic decomposition of water [12]. However, the sulfide ion is readily oxidized to sulfate by the photogenerated holes, with Cd^{2+} ions escaping into the solution. Use of sulfides as electron donors diminishes the photocorrosion of the catalyst [4–6]. A possible way of enhancing the photocatalytic activity of cadmium sulfide is to develop composite materials based on CdS and broader band semiconductors, for example, ZnS [13]. Zinc and cadmium sulfides have similar crystal structures, so they fairly readily form $Cd_{1-x}Zn_xS$ solid solutions. In addition, use of these systems is profitable from the practical standpoint, since they are obtained from rather cheap precursors. The band gap can easily be varied by changing the molar ratio of the components [1]. Efficient hydrogen evolution on the sulfide photocatalysts $Cd_{1-x}Zn_xS$ is attainable without adding noble metals [14], which makes it possible to decrease the cost of the materials.

In the present work, we propose a two-step method for preparation of cadmium–zinc mixed sulfides with a large specific surface area and developed porous structure. This method was used earlier in the synthesis of pure cadmium sulfide [15]:

$$CdCl_2 + 2NaOH = Cd(OH)_2 + 2NaCl, \quad (IV)$$

$$ZnCl_2 + 2NaOH = Zn(OH)_2 + 2NaCl, \quad (V)$$

$$(1-x)Cd(OH)_2 + xZn(OH)_2 + Na_2S = Cd_{1-x}Zn_xS + 2NaOH. \quad (VI)$$

The activity of the synthesized materials was estimated in the photocatalytic hydrogen evolution from aqueous solutions of sodium sulfide and sodium sulfite ($\lambda > 420$ nm). that the highest activity was shown by $Cd_{0.3}Zn_{0.7}S$, whose band gap is $E_g = 2.71$ eV. We stud-

ied the influence of the catalyst concentration, pH, and the initial substrate concentration on the rate of photocatalytic hydrogen evolution. A decrease in the pH from 12.5 to 6.5 increased the hydrogen evolution rate by a factor of approximately 2. At optimal process parameters, the quantum efficiency of photocatalytic hydrogen evolution was up to 12.9%, which is a large value for a process occurring under irradiation with visible light on a catalyst containing no noble metal.

EXPERIMENTAL

Photocatalyst Synthesis

The chemicals—Na_2S (high-purity grade), Na_2SO_3 (analytical grade), NaOH (analytical grade), H_2SO_4 (analytical grade), $CdCl_2$ (analytical grade), and $ZnCl_2$ (analytical grade)—were used as received. Distilled water further purified in an Easy pure II system was used in all experiments.

The composite photocatalysts $Cd_{1-x}Zn_xS$ were synthesized as follows. A heat-resistant 500-mL beaker containing a 0.1 M NaOH solution (100 mL) was placed on a magnetic stirrer, and a mixed solution (100 mL) of cadmium chloride and zinc chloride in proportions corresponding to $x = 0$, 0.3, 0.7, 0.9, 0.95, or 1.0 was added. Precipitation was carried out with a 0.1 M Na_2S solution at a twofold excess of sodium sulfide. The mixture was then stirred for 20 min. The resulting suspension was placed in Teflon beakers and centrifuged. The precipitate was washed with distilled water about 10 times. Thereafter, the precipitate was decanted and was kept in a drying oven at 70°C for 15 h.

Properties of the Materials

The semiconductor catalysts were characterized by a complex of physicochemical methods: X-ray diffraction, low-temperature adsorption of nitrogen, transmission electron microscopy (TEM), and diffuse reflectance spectroscopy of (DRS).

X-ray diffraction patterns were obtained on an ARL X'TRA X-ray diffractometer (semiconductor detector, CuK_α radiation, $\lambda_{av} = 1.54178$ Å, anode voltage of 45 kV, anode current of 35 mA). Textural characteristics (specific surface area S_{sp} and specific pore volume V_{pore}) were determined by low-temperature nitrogen adsorption using an Autosorb-6B analyzer (Quantachrome). The surface properties of the catalysts were studied by energy dispersive X-ray microanalysis using an EDAX energy dispersive spectrometer (Phoenix) and a JEM-2010 high-resolution transmission electron microscope (JEOL). Diffuse reflectance spectra were recorded on a Lambda 35 UV-VIS spectrometer (PerkinElmer) with an RSA-PE-20 diffuse reflectance attachment (Labsphere).

Catalytic Activity Measurements

The setup for studying the photocatalytic evolution of hydrogen was described earlier [16]. An aqueous suspension of a $Cd_{1-x}Zn_xS$ catalyst in a solution containing Na_2S (0.05–0.3 mol/L) and Na_2SO_3 (0.02 mol/L), in a sealed temperature-controlled reactor, was irradiated with a DRSh-1000 lamp under continuous stirring. A ZhS-11 light filter was used to cut off the wavelengths shorter than 420 nm. A 1 M sulfuric acid or 0.1 M sodium hydroxide solution was added to change the pH. The catalyst content was varied between 0.05 and 1.54 g/L. The reactor was preliminarily purged with argon for 20 min so as to remove the entire oxygen. The presence or absence of oxygen was checked by gas chromatography. The evolved hydrogen was quantified on an LKhM-8-MD gas chromatograph. The radiation power between 420 and 600 nm was 0.008 W/cm^2. In this wavelength range, the emission spectrum of the DRSh-1000 mercury lamp has three peaks at 440, 555, and 585 nm with a relative intensity of 39, 38, and 23%, respectively. The number of photons emitted per unit time was calculated as

$$NS = N_{\text{phot}}\varphi_i\sum_i h\frac{c}{\lambda_i}, \qquad (1)$$

where S is the light spot area (3.8 cm^2), N is the radiation power, λ_i is the ith peak wavelength, φ_i is the relative intensity of the ith peak, N_{phot} is the number of photons, and $h\frac{c}{\lambda_i}$ is the energy of a light quantum. It turned out that $N_{\text{phot}} = 7.79 \times 10^{16}$ photon/s or 1.29×10^{-7} E/s. The quantum efficiency (%) was calculated using the equation

$$\phi = \left(2w_0(H_2)/N_{\text{phot}}\right) \times 100, \qquad (2)$$

where $w_0(H_2)$ is the initial rate of photocatalytic hydrogen evolution. The coefficient 2 means that two electrons are necessary for the formation of a hydrogen molecule, and, correspondingly, it is required that two photons interact with the catalyst [17].

RESULTS AND DISCUSSION

Characteristics of the Photocatalysts

X-ray diffraction study of $Cd_{1-x}Zn_xS$. The X-ray diffraction patterns of a series of $Cd_{1-x}Zn_xS$ samples prepared via the above procedure are shown in Fig. 1. The phase composition and crystallite size data for the samples are listed in the table.

The diffraction patterns of the samples with Cd : Zn = 7 : 3, 1 : 1, 3 : 7, 1 : 9, and 1 : 19 at the synthesis stage (x = 0.3, 0.5, 0.7, 0.9, and 0.95, respectively) exhibit only reflections from the $Cd_{1-x}Zn_xS$ solid solution. The first peak shifts gradually to larger angles with an increasing Zn content. An analysis of the peak positions suggests that the composition of the samples with x = 0.3–0.95 is in agreement with the

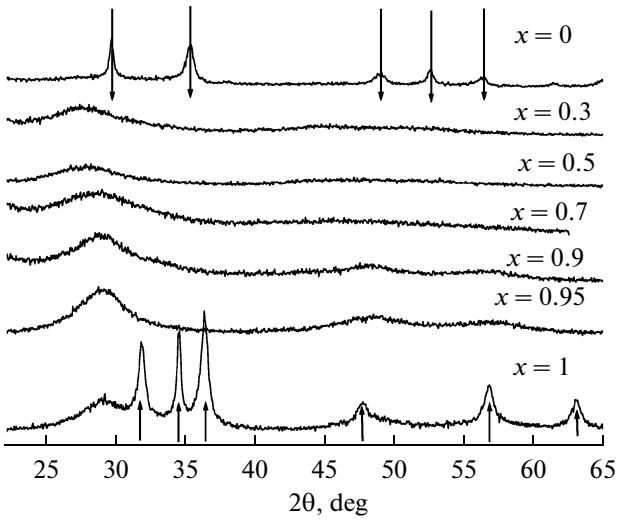

Fig. 1. X-ray diffraction patterns of $Cd_{1-x}Zn_xS$ samples. Designations: ↓ is $Cd(OH)_2$ and ↑ is ZnO.

initial proportions of $CdCl_2$ and $ZnCl_2$ taken for the synthesis. The crystallite size of the $Cd_{1-x}Zn_xS$ particles with $x = 0.3$–0.9 is smaller than 2 nm, whereas the crystallite size of $Cd_{0.05}Zn_{0.95}S$ is 2.2 nm. The diffraction pattern of the $Cd_{1-x}Zn_xS$ sample in which the mole fraction of cadmium is assumed to be 100% contains only reflections from cadmium hydroxide with a crystallite size of about 15 nm. This is likely due to the CdS particles being amorphous to X-rays. The diffraction pattern of the sample with a zinc mole fraction of 100% at the synthesis stage indicates the presence of zinc oxide with a crystallite size of 20 nm, and the ZnS particles of this sample have a crystallite size of 2.2 nm. Because of the strong broadening of the peaks, it is impossible to determine whether the structure of the solid solution is hexagonal or cubic.

Under the assumption that the structure is cubic (sphalerite-like), the interplanar spacing d_{111} can be derived from the position of the first peak (2θ) using the Wolf–Bragg equation

$$d = \frac{\lambda}{2\sin\theta}, \quad (3)$$

where λ = 1.5418 Å is the wavelength of the CuK_α X-ray radiation. The cubic unit cell parameter a was calculated as

$$a = d_{hkl}\sqrt{h^2 + k^2 + l^2} = d_{111}\sqrt{3}, \quad (4)$$

where h, k, and l are the Miller indices that specify the crystallographic reflection planes.

The dependence of the cubic unit cell parameter a on x is shown in Fig. 2. The monotonic decrease in a indicates the formation of a CdS–ZnS solid solution. However, the unit cell parameters are substantially smaller than the tabulated values of a = 5.818 Å for CdS (PDF#421411) and a = 5.406 Å for ZnS (PDF#050566). These discrepancies can be attributed to the fact that the defect concentration in our samples is very high and, accordingly, the structure cannot be considered purely cubic. It is most likely that the synthesized samples contain elements of both cubic and hexagonal structures. It was earlier shown that both modifications of the catalyst can be used in the photocatalytic production of hydrogen [14, 17, 18].

Diffuse reflectance spectra of the catalysts based on cadmium and zinc sulfides. The DRS spectra of the synthesized samples were recorded in order to calculate the position of the absorption band edge for the catalysts. The band gap for direct-gap semiconduc-

Physicochemical properties and catalytic activity of the photocatalysts based on cadmium and zinc sulfides

Phase composition	Crystallite size, nm	E_g, eV	λ, nm	S_{sp}, m^2/g	V_{pore}, cm^3/g	$w_0(H_2)$, μmol/min	ϕ, %
$Cd(OH)_2$	15	2.39	518	84.9	0.46	0.043	1.11
CdS	*						
$Cd_{0.7}Zn_{0.3}S$	<2	2.42	512	111.6	0.63	0.110	2.84
$Cd_{0.5}Zn_{0.5}S$	<2	2.60	477	111.3	0.43	0.138	3.57
$Cd_{0.3}Zn_{0.7}S$	<2	2.71	456	156.0	0.42	0.290	7.49 (12.9)**
$Cd_{0.1}Zn_{0.9}S$	<2	2.89	429	228.5	0.24	0.160	4.13
$Cd_{0.05}Zn_{0.95}S$	2.2	3.00	413	204.0	0.21	0.062	1.60
ZnO	20	3.30	376	88.0	0.32	0.015	0.39
ZnS	2.2						

Note: Reaction conditions: 20°C, $[Na_2S]_0$ = 0.1 mol/L, $[Na_2SO_3]_0$ = 0.02 mol/L, catalyst content of 0.77 g/L, pH 12.5, and suspension volume of 65 mL.

* The particles are amorphous to X-rays.

** Catalyst content of 1.15 g/L, pH 8.3.

tors, including cadmium and zinc sulfides, is calculated using the Tauc formula [19]. Initially, the adsorption coefficient $F(R)$ is determined from diffuse reflectance data using the Kubelka–Munk equation

$$F(R) = \frac{(1-R)^2}{2R}, \quad (5)$$

where R is the reflectance of the sample. Next, curves in the Tauc coordinates are plotted. The plots for our samples are presented in Fig. 3a. The band gap is calculated by constructing a tangent to the curves and by finding the X axis intercept for this tangent. Figure 3b illustrates the construction of this tangent by the example of the $Cd_{0.1}Zn_{0.9}S$ catalyst. This line intersects the abscissa axis at the $x \approx 2.9$ eV point. The Tauc plot for the $CdS/Cd(OH)_2$ sample proves that this sample contains cadmium sulfide, for the absorption band edge for this catalyst is near 2.3 eV, whereas pure $Cd(OH)_2$ is a white substance and its absorption edge should lie in the UV range. The band gap of zinc oxide in the ZnS–ZnO composite is 3.2 eV [20] and that of zinc oxide ranges from 3.5 eV for the cubic structure to 3.9 eV for the hexagonal structure [21, 22]. Thus, the curve in Fig. 3a, with the calculated absorption band edge of about 3.3 eV, can be the superposition of the diffuse reflectance curves of zinc sulfide and zinc oxide in the Tauc coordinates. The band gap decreases from 3.00 to 2.42 eV as x in $Cd_{1-x}Zn_xS$ increases from 0.05 to 0.7. These values are in good agreement with the results of previous studies [17, 22].

Textural characteristics of the $Cd_{1-x}Zn_xS$ materials. The textural characteristics of the synthesized samples were studied by low-temperature nitrogen adsorption. The S_{BET} and V_{pore} data obtained are listed in the table. The specific surface area of $Cd_{1-x}Zn_xS$ increases with an increasing the zinc content of the material. The ZnO–ZnS and $Cd(OH)_2/CdS$ samples have the smallest specific surface areas, and $Cd_{0.1}Zn_{0.9}S$ is characterized by the largest S_{BET} value of 228 m^2/g. It was demonstrated earlier that S_{BET} as a function of x passes through a maximum, the $Cd_{1-x}Zn_xS$ samples with $x = 0.56–0.9$ have a large specific surface area [10, 14, 23–25], and the largest specific surface area of 190 m^2/g is observed for $Cd_{0.2}Zn_{0.8}S$ [14] obtained by coprecipitating zinc and cadmium acetates with thiourea followed by heating. Pure cadmium sulfide synthesized by a two-step method via cadmium hydroxide precipitation had $S_{BET} = 113$ m^2/g [15]. Thus, our S_{BET} versus x data are in good agreement with the published data. In addition, the specific surface area of $Cd_{0.1}Zn_{0.9}S$ is larger than those of the samples synthesized and described previously [10, 14, 15, 23–25]. The sulfides synthesized in this study have rather large specific pore volumes (0.24–0.63 cm^3/g). This is favorable for attaining a higher rate of the liquid-phase photocatalytic reaction.

TEM study of the samples based on cadmium sulfide and zinc sulfide. The images of the $Cd_{0.7}Zn_{0.3}S$ catalyst are shown in Fig. 4. As can be seen, the sample consists of compressed nanotubes or hollow spheres with a diameter of approximately 50 nm and a wall thickness of 5–8 nm. However, the coherently scattering domains do not exceed 2–5 nm, which agrees well with the X-ray diffraction data. The formation of these structures is due to the fact that the synthesis consisted of two steps. The first step yields large, piled hydroxide particles (~50 nm). The second step is the interaction of the hydroxide with sodium sulfide, which yields hollow nanotubes of cadmium sulfide [15]. The images shown in Fig. 4 resemble the images of CdS catalysts presented by Bao et al. [15], whose work was used as the basis for our syntheses.

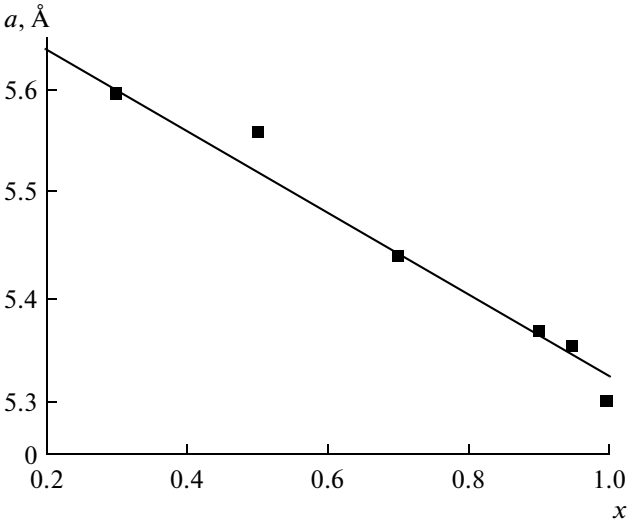

Fig. 2. Dependence of the cubic unit cell parameter a on the mole fraction of zinc in $Cd_{1-x}Zn_xS$.

Kinetics of the Photocatalytic Evolution of Hydrogen

Dependence of the hydrogen evolution rate on the zinc-to-cadmium ratio. The $Cd_{1-x}Zn_xS$ catalysts with $x = 0.56–0.9$ were demonstrated to be the most active in the photocatalytic evolution of hydrogen from aqueous Na_2S/Na_2SO_3 solutions [10, 14, 17, 22–25], and most researchers believe that the optimum mole fraction of zinc is >65% [17, 22–25]. Figure 5 plots the initial rates of photocatalytic hydrogen evolution, $w_0(H_2)$, for catalysts based on cadmium and zinc sulfides with different mole fractions of the components.

The plot of $w_0(H_2)$ versus x passes through a maximum. The $x = 0$ and $x = 1$ samples show the lowest activity. The absorption edges of the ZnS–ZnO and $Cd_{0.05}Zn_{0.95}S$ samples occur at 376 and 413 nm. Therefore, when the filter cutting off the wavelengths shorter than 420 nm is used, the photocatalytic reaction cannot ensure efficient hydrogen evolution. The addition of a broader band semiconductor, such as zinc sulfide, to cadmium sulfide shifts the absorption edge to shorter wavelengths. As a consequence, the accessible fraction of the emission spectrum of the

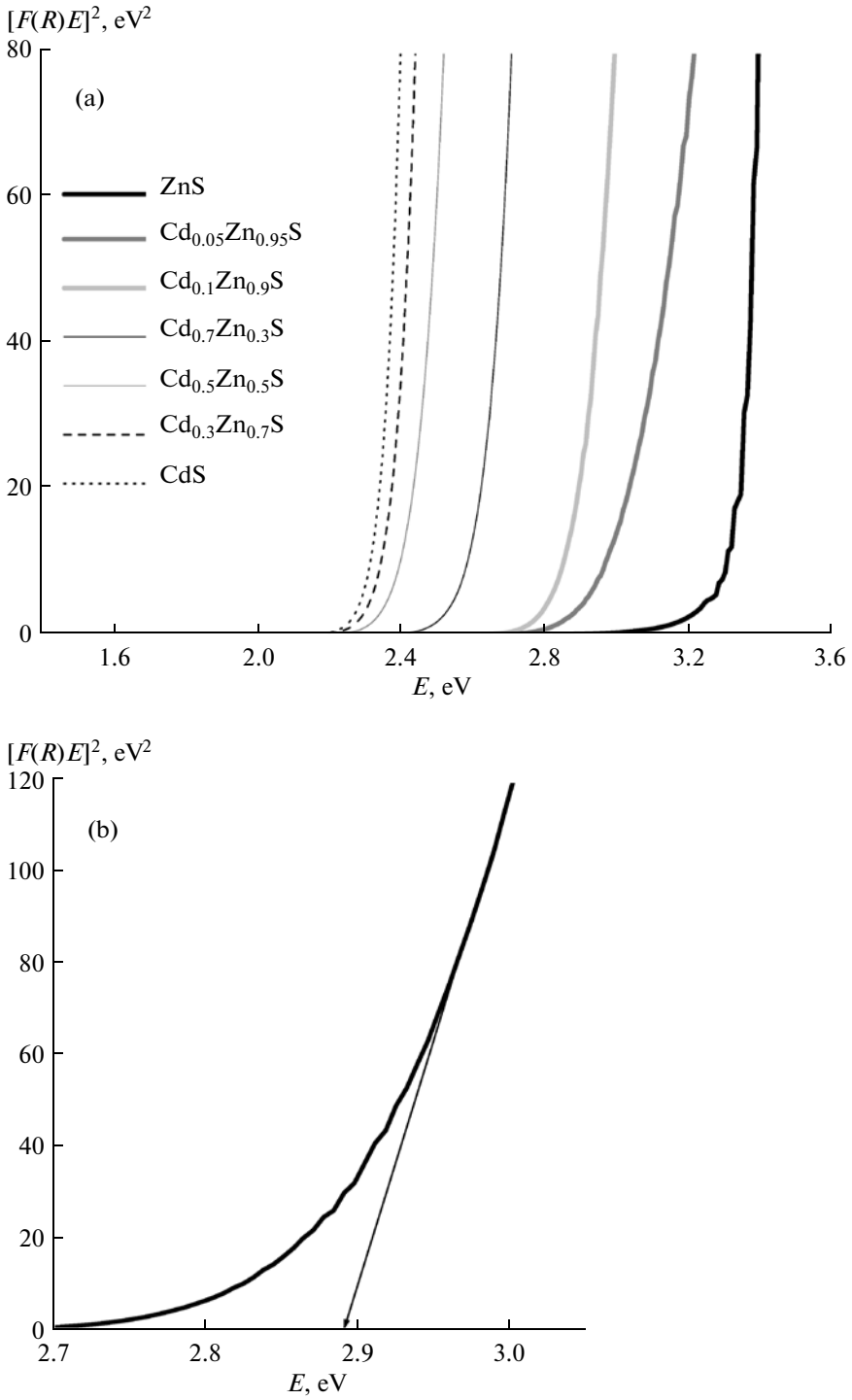

Fig. 3. (a) Diffuse reflectance spectra of the synthesized catalysts based on cadmium and zinc sulfides and (b) construction of the tangent to the curve for $Cd_{0.1}Zn_{0.9}S$.

source decreases and so does the rate of electron and hole formation via Eq. (I). Therefore, the rate of photocatalytic hydrogen evolution should also decrease [17]. However, the hydrogen evolution efficiency depends on the band gap width and also on the energy of the electrons of the conduction band (E_{CB}). The addition of zinc sulfide to cadmium sulfide increases E_{CB}, and this results in an increase in the reductive power of the photogenerated electrons and in an increase in the rate of hydrogen formation via reaction (II) [17]. The synthesis of $Cd_{1-x}Zn_xS$ solid solutions with a controllable band gap and with a preset position

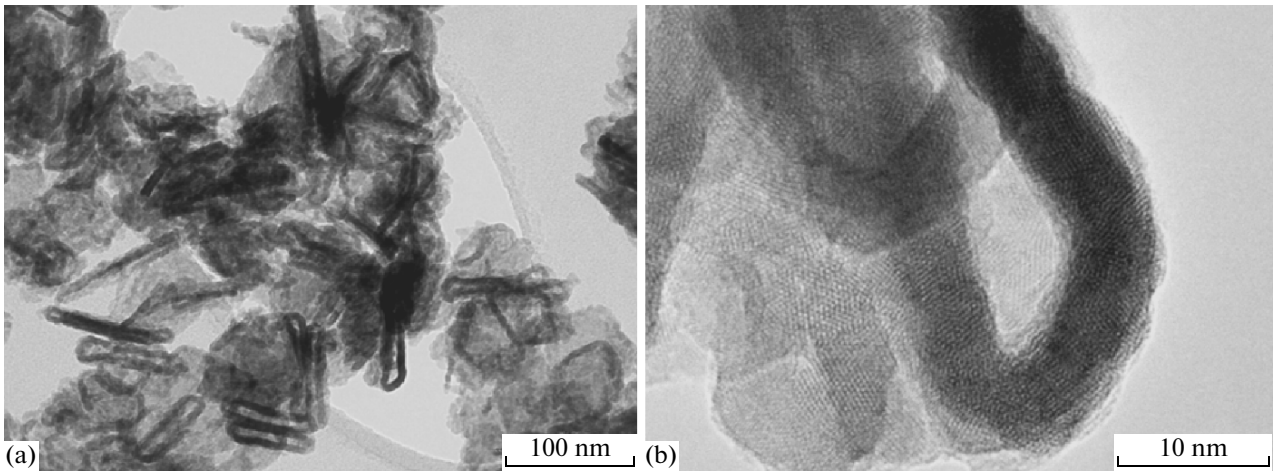

Fig. 4. Electron micrographs of the synthesized $Cd_{0.3}Zn_{0.7}S$ catalyst. Scales: (a) 100 nm and (b) 10 nm.

of the conduction band makes it possible to achieve a balance between the efficient light absorption and high reductive power. This allows one to develop catalysts that are much more active under irradiation with visible light than pure cadmium sulfide [10, 14, 22–24]. In our work, the $Cd_{0.3}Zn_{0.7}S$ catalyst turned out to be optimal. In other works in which different methods of synthesis were used [17, 22] the optimal values of x varied widely, implying variation of the phase composition, particle shape and size, and defect concentration, which are strong factors governing the optical transitions in the semiconductor catalysts and, hence, the rate of the photocatalytic reaction.

Dependence of the hydrogen evolution rate on the catalyst content. After the most active photocatalyst was determined ($Cd_{0.3}Zn_{0.7}S$), we studied the dependence of the hydrogen evolution rate on the catalyst concentration (C_{Cat}).

In the determination of the most active catalyst, the $Cd_{0.3}Zn_{0.7}S$ content was 0.77 g/L. In subsequent experiments, C_{Cat} was varied between 0 and 1.54 g/L. The dependence of $w_0(H_2)$ on C_{Cat} is shown in Fig. 6a, and Fig. 6b plots the hydrogen evolution rate per unit weight of the catalyst. The rate $w_0(H_2)$ increases almost linearly as C_{Cat} is increased from 0 to 0.38 g/L (Fig. 6a), and, as the concentration is raised to 1.15 g/L, the hydrogen evolution rate curve flattens out. It was demonstrated in earlier works [15, 26] that, in the case of pure cadmium sulfide, the highest rate of photocatalytic hydrogen evolution per gram of catalyst is attained at a sulfide concentration of 0.25–0.75 g/L, which is considerably higher than the corresponding value obtained in the present work (0.046 g/L). This can be explained by the fact that light sources with a higher radiation intensity were used in the previous studies [15, 26]. The shape of the curves plotted in Figs. 6a and 6b is determined by the fact that light absorption is proportional to the number of $Cd_{0.3}Zn_{0.7}S$ particles at low concentrations of the photocatalyst. With an increase in the concentration of absorbing particles, the suspension becomes opaque, light penetration into the solution is hampered, and the rate of the photocatalytic reaction stops increasing [27]. The subsequent experiments were conducted at a catalyst concentration of 1.15 g/L for the reason that this concentration ensures attaining the maximum absolute rate of photocatalytic hydrogen evolution and efficient light absorption.

Dependence of the hydrogen evolution rate on the pH of the solution. The influence of the addition of

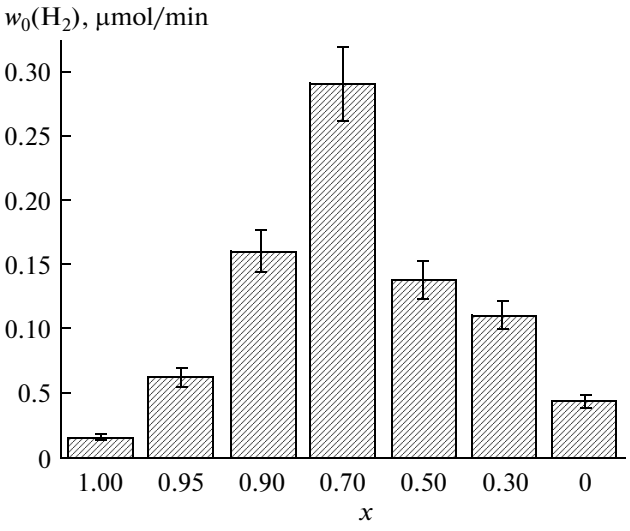

Fig. 5. Initial rates of photocatalytic hydrogen evolution from aqueous Na_2S–Na_2SO_3 solutions in the presence of $Cd_{1-x}Zn_xS$ catalysts. The $x = 0$ and $x = 1$ catalysts contain impurities (see the table). Reaction conditions: 20°C, $[Na_2S]_0 = 0.1$ mol/L, $[Na_2SO_3]_0 = 0.02$ mol/L, catalyst content of 0.77 g/L, pH 12.5, and suspension volume of 65 mL.

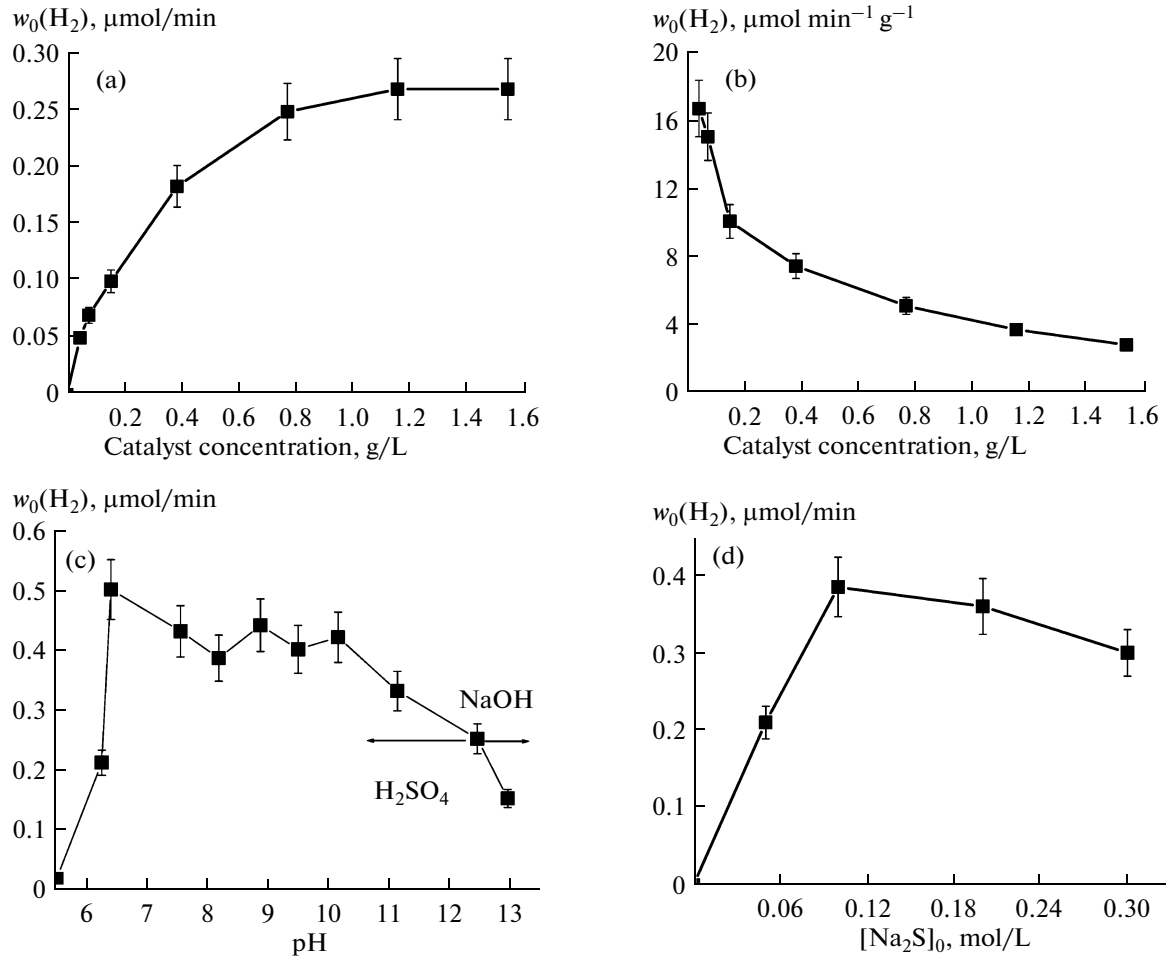

Fig. 6. Plots of (a) $w_0(H_2)$ and (b) $w_0(H_2)$ per unit weight of the catalyst versus the $Cd_{0.3}Zn_{0.7}S$ content, (c) versus the initial value of pH, and (d) versus the initial Na_2S concentration. Reaction conditions: (a–d) 20°C, (a–c) $[Na_2S]_0 = 0.1$ mol/L, (a–d) $[Na_2SO_3]_0 = 0.02$ mol/L, (a–d) suspension volume of 65 mL, (c, d) $Cd_{0.1}Zn_{0.9}S$ content of 1.15 g/L, (a, b) pH 12.5, (d) pH 8.3.

sodium hydroxide to the reaction mixture and of the corresponding change in the solution pH on the hydrogen evolution rate was studied earlier [26]. In experiments on the $Cd_{0.3}Zn_{0.7}S$ photocatalyst, the initial value of pH was varied between 5.5 and 13 by adding 1 M H_2SO_4 or 0.1 M NaOH. The addition of alkali decreases $w_0(H_2)$ (Fig. 6c). As the pH of the solution is decreased down to pH 6.5 by adding sulfuric acid, the rate of photocatalytic hydrogen evolution increases monotonically, and it decreases sharply once pH 6.5 is reached. This is due to the fact that the following redox reaction occurs in the acidic medium to form elemental sulfur from the sulfide:

$$3Na_2S + 4H_2SO_4 \longrightarrow 4S^0 + 3Na_2SO_4 + 4H_2O. \quad \text{(VII)}$$

The formation of elemental sulfur is proved by the solution turning yellow after the addition of an excess of 1 M H_2SO_4 followed by the precipitation of a white substance.

To understand why the reaction rate increases on passing from alkaline pH values to neutral ones, we considered the mechanism of photocatalytic hydrogen production in aqueous sodium sulfide + sodium sulfite solutions. In the absence of sodium sulfite, the following main reactions occur [22, 26]:

$$CdS + h\nu \longrightarrow CdS + h^+ + e^-, \quad \text{(VIII)}$$

$$2S^{2-} + 2h^+ \longrightarrow S_2^{2-} \quad \text{(IX)}$$

accompanied by the evolution of hydrogen via reaction (II). The following reaction occurs in the system upon the addition of sodium sulfite:

$$S_2^{2-} + SO_3^{2-} \longrightarrow S_2O_3^{2-} + S^{2-}. \quad \text{(X)}$$

The overall reaction can be described by the equation

$$Na_2S + Na_2SO_3 + 2H_2O \longrightarrow H_2 + Na_2S_2O_3 + 2NaOH. \quad \text{(XI)}$$

Thus, according to reaction (II), an increase in the concentration of hydroxyl ions thermodynamically hampers the hydrogen evolution reaction [22, 26], whereas a decrease in the solution pH increases the reaction rate. The effect of an acid on the photocata-

lytic evolution of hydrogen in the Na_2S–Na_2SO_3 system was not studied earlier. The solution pH was changed only by varying the Na_2S concentration and by adding NaOH, and no noticeable increase in the reaction rate was observed [15, 26, 28].

Influence of the substrate concentration on the hydrogen evolution rate. Another purpose of our study was to correlate the rate of photocatalytic hydrogen evolution with the initial concentration of the electron donor (sodium sulfide). This factor was varied without changing the other parameters of the system, including pH. For this reason, the solution in all experiments initially had pH 8.3, which was established by addition of 1 M H_2SO_4. The dependence of $w_0(H_2)$ on the initial concentration of sodium sulfide is shown in Fig. 6d.

The maximum rate of photocatalytic hydrogen evolution is observed at a sodium sulfide concentration of 0.1 mol/L. In most works on the photocatalytic evolution of hydrogen in the sulfide–sulfite system with a catalyst based on cadmium sulfide, $[Na_2S]_0$ ranged from 0.1 to 0.3 mol/L [10, 14, 22, 26]. It can be seen from Fig. 6d that, with an increase in the Na_2S concentration, $w_0(H_2)$ first increases and begins to decrease slowly above 0.1 mol/L. It is believed that the potential of the conduction band of cadmium sulfide in the suspension changes with an increasing sodium sulfide concentration, which decreases the rate of photocatalytic hydrogen evolution [15]. The negatively charged anions of sodium sulfide are adsorbed on the catalyst surface. As a consequence, an electron requires more energy to reach the surface and this lowers the efficiency of the process.

Under the optimal conditions for the photocatalytic reaction ($[Na_2S]_0 = 0.1$ mol/L, $Cd_{0.3}Zn_{0.7}S$ concentration of 1.15 g/L), the quantum efficiency is 12.9%. This value is very large for the noble metal–free photocatalysts based on cadmium and zinc sulfides. Earlier, the maximum quantum efficiency attained in these systems varied between 2.17 and 10.23% [10, 14, 17, 23, 24].

Thus, in the present work, we used a two-step method to synthesize noble metal–free $Cd_{1-x}Zn_xS$ photocatalysts from zinc and cadmium chlorides via hydroxide formation as the intermediate step. The catalysts have been characterized by a complex of physicochemical methods (X-ray diffraction, DRS, TEM, and low-temperature nitrogen adsorption). The synthesized samples were tested in photocatalytic hydrogen evolution from aqueous solutions of sodium sulfide and sodium sulfite under irradiation with visible light ($\lambda > 420$ nm). The $Cd_{0.3}Zn_{0.7}S$ sample, which has a band gap of 2.71 eV, a specific surface area of 56 m^2/g, and a specific pore volume of 0.42 cm^3/g, exhibits the highest activity. The maximum rate of photocatalytic hydrogen evolution was attained at an initial sodium sulfide concentration of 0.1 mol/L, a catalyst content of 1.15 g/L, and pH 6.5. Passing from pH 12.5 to pH 6.5 causes an approximately twofold increase in the hydrogen evolution rate. Under the optimal conditions, the quantum efficiency of photocatalytic hydrogen evolution is 12.9%, which exceeds the values reported for similar systems.

ACKNOWLEDGMENTS

The authors are grateful to A.V. Vorontsov for assistance in interpreting experimental data and to S.V. Cherepanova, E.Yu. Gerasimov, and T.Ya. Efimenko for taking part in the physicochemical study of the samples.

This work was supported through the Federal Target Program "Scientific and Scientific–Pedagogical Personnel of Innovative Russia" (state contract no. P130 of June 11, 2010) and by the President of the Russian Federation through the Leading Scientific Schools Program (grant no. NSh-3156.2010.3).

REFERENCES

1. Zamaraev, K.I. and Parmon, V.N., *Catal. Rev. Sci. Eng.,* 1980, vol. 22, no. 2, p. 261.
2. Savinov, E.N., *Cand. Sci. (Chem.) Dissertation,* Novosibirsk: Boreskov Inst. of Catalysis, 1982.
3. Savinov, E.N., *Doctoral (Chem.) Dissertation*, Novosibirsk: Boreskov Inst. of Catalysis, 1993.
4. Gruzdkov, Yu.A., Savinov, E.N., and Parmon, V.N., *Khim. Vys. Energ.*, 1986, vol. 20, no. 5, p. 445.
5. Gruzdkov, Yu.A., Savinov, E.N., and Parmon, V.N., *Kinet. Katal.*, 1986, vol. 27, no. 1, p. 133.
6. Gruzdkov, Yu.A., Savinov, E.N., and Parmon, V.N., *Khim. Fiz.*, 1988, vol. 7, no. 1, p. 44.
7. Li, Y.X., Lu, G.X., and Li, S.B., *Appl. Catal., A*, 2001, vol. 214, no. 2, p. 179.
8. Fedoseev, V.I., Savinov, E.N., and Parmon, V.N., *Kinet. Katal.,* 1987, vol. 28, no. 5, p. 1111.
9. Tsuji, I., Kato, H., Kobayashi, H., and Kudo, A., *J. Am. Chem. Soc.*, 2004, vol. 126, no. 41, p. 13406.
10. Xing, C.J., Zhang, Y.J., Yan, W., and Guo, L.J., *Int. J. Hydrogen Energy*, 2006, vol. 31, no. 14, p. 2018.
11. Ren, L., Yang, F., Deng, Yu., Yan, N., Huang, Sh., Lei, D., Sun, Q., and Yu, Y., *Int. J. Hydrogen Energy*, 2010, vol. 35, no. 8, p. 3297.
12. Zhu, J. and Zach, M., *Curr. Opin. Colloid. Interface Sci.,* 2009, vol. 14, no. 4, p. 260.
13. Chen, J., Lin, Sh., Yan, G., Yang, L., and Chen, X., *Catal. Commun.*, 2008, vol. 9, no. 1, p. 65.
14. Zhang, W. and Xu, R., *Int. J. Hydrogen Energy*, 2009, vol. 34, no. 20, p. 8495.
15. Bao, N.Z., Shen, L.M., Takata, T., and Domen, K., *Chem. Mater.*, 2008, vol. 20, no. 1, p. 110.
16. Kozlova, E.A. and Vorontsov, A.V., *Int. J. Hydrogen Energy*, 2010, vol. 35, no. 14, p. 7337.
17. Zhang, K., Jing, D., Xing, C., and Guo, L., *Int. J. Hydrogen Energy*, 2007, vol. 32, no. 18, p. 4685.

18. Biswas, S., Kar, S., Santra, S., Jompol, Y., Arif, M., and Khondaker, S.I., *J. Phys. Chem. C*, 2009, vol. 113, no. 9, p. 3617.
19. Xu, X., Lu, R., Zhao, X., Xu, S., Lei, X., Zhang, F., and Evans, D.G., *Appl. Catal., B*, 2011, vol. 102, nos. 1–2, p. 147.
20. Jing, D., Guo, L., Zhao, L., Zhang, X., Liu, H., Li, M., Shen, Sh., Liu, G., Hu, X., Zhang, X., Zhang, K., Ma, L., and Guo, P., *Int. J. Hydrogen Energy*, 2010, vol. 35, no. 13, p. 7087.
21. Fang, X., Zhai, T., Gautam, U.K., Li, L., Wu, L., Bando, Y., and Golberg, D., *Prog. Mater. Sci.*, 2011, vol. 56, no. 2, p. 175.
22. Wang, L., Wang, W., Shang, M., Yin, W., Sun, S., and Zhang, L., *Int. J. Nydrogen Energy*, 2010, vol. 35, no. 1, p. 19.
23. Zhang, K., Jing, D., Liu, M., and Guo, L., *Catal. Commun.*, 2008, vol. 9, no. 8, p. 1720.
24. Zhang, K., Jing, D., and Guo, L., *Int. J. Hydrogen Energy*, 2010, vol. 35, no. 13, p. 7051.
25. Zhang, K., Jing, D., Chen, Q., and Guo, L., *Int. J. Hydrogen Energy*, 2010, vol. 35, no. 5, p. 2048.
26. Sabate, J., Cervera-March, S., Simmaro, R., and Gimenez, J., *Chem. Eng. Sci.*, 1990, vol. 45, no. 10, p. 3089.
27. Carp, O., Huisman, C.L., and Reller, A., *Prog. Solid State Chem.*, 2004, vol. 32, nos. 1–2, p. 33.
28. Sahu, N., Upadhyay, S.N., and Sinha, A.S.K., *Int. J. Hydrogen Energy*, 2009, vol. 34, no. 1, p. 130.